

Quantum-interference resonant photocurrent

A. P. Dmitriev, S. A. Emel'yanov, Ya. V. Terent'ev, and I. D. Yaroshetskii

A. F. Ioffe Physicotechnical Institute, Academy of Sciences of the USSR, Leningrad
(Submitted 27 July 1990)

Zh. Eksp. Teor. Fiz. **99**, 619–640 (February 1991)

A detailed analysis is given of a recently discovered new physical effect in the form of a quantum-interference resonant photocurrent [A. P. Dmitriev, S. A. Emel'yanov, Ya. V. Terent'ev, and I. D. Yaroshetskii, JETP Lett. **49**, 584 (1989); **51**, 445 (1990); Solid State Commun. **72**, 1149 (1989)]. This effect may appear under the influence of light in a great variety of media both with and without a center of inversion (symmetry). A necessary condition is the existence of an energy level interacting with states in the continuous spectrum of a medium. The photocurrent is not a consequence of a familiar quantum-interference effect which occurs under absorption conditions and is known as the Fano resonance. It is shown that the photocurrent has the following characteristic features: its direction is reversed on passage through the point of resonance and, in the region where the offset Δ from the resonance is greater than the width of the level, it decreases as $1/\Delta$; the resonance amplitude may exceed the background even when the corresponding optical transition is almost forbidden. A theory of the effect is developed and examples of physical systems in which it can be observed are given.

INTRODUCTION

If the energy spectrum of a physical system includes a discrete level interacting with states in the continuous spectrum of the system, then the frequency dependence of the optical absorption coefficient α may exhibit an asymmetric peak known as the Fano resonance.³ This antisymmetric Fano correction to the main Lorentzian absorption profile is inversely proportional to the offset (detuning) Δ from a resonance and is due to quantum interference of optical transitions to the continuous spectrum.

We show that the presence of a level interacting with the continuous spectrum gives rise to a new effect in the form of a quantum-interference resonant drift of carriers (photocurrent). This photocurrent is unrelated to the Fano correction to the absorption coefficient and, in particular, it may appear when the latter is altogether absent.

We illustrate this by means of the scheme shown in Fig. 1. Under the action of an optical photon of energy $\hbar\omega$ an electron could be transferred from an initial state 1 to a final state 3 belonging to the continuous spectrum either directly ($1 \rightarrow 3$) or via an intermediate state 2 corresponding to a discrete level ($1 \rightarrow 2 \rightarrow 3$). We denote the amplitudes of the two transitions by P_k and R_k . The $1 \rightarrow 2 \rightarrow 3$ transition is resonant and its amplitude is $R_k = Q_{12} V_k / \Delta$, where Q_{12} and V_k are the matrix elements of the $1 \rightarrow 2$ and $2 \rightarrow 3$ transitions from the level to the continuous spectrum, while $\Delta = \epsilon_k - \epsilon_2$ is the difference between the energies of the final and intermediate states, which is equal to the offset $\hbar\omega - (\epsilon_2 - \epsilon_1)$ from a resonance. The total transition probability W_k to a state with a momentum k is proportional to $|P_k + R_k|^2$.

In the simplest case of an isotropic energy band, we find that

$$\alpha \propto \sum_{\mathbf{k}} W_{\mathbf{k}} \propto \sum_{\mathbf{k}} |P_{\mathbf{k}}|^2 + \sum_{\mathbf{k}} |R_{\mathbf{k}}|^2 + 2 \sum_{\mathbf{k}} \text{Re}(P_{\mathbf{k}} R_{\mathbf{k}}^*), \quad (1)$$

where the summation is carried out over all the directions of the momentum k . The first term on the right-hand side of Eq. (1) represents the nonresonant contribution to the ab-

sorption. The second term is Lorentzian $|Q_{12}|^2 |V_k|^2 / \Delta^2$ and describes the absorption by the level 2 followed by decay to the band of the resultant quasistationary state. The third term is the above-mentioned antisymmetric interference correction to α . It differs from zero if the part of $\text{Re}(P_k R_k^*)$ even with respect of the momentum does not vanish.

We now consider the problem of the photocurrent which may appear in such a system. In general, it is proportional to the total momentum of the optically excited carriers:

$$j \propto \sum_{\mathbf{k}} \mathbf{k} W_{\mathbf{k}} \propto \sum_{\mathbf{k}} \mathbf{k} |P_{\mathbf{k}}|^2 + \sum_{\mathbf{k}} \mathbf{k} |R_{\mathbf{k}}|^2 + 2 \sum_{\mathbf{k}} \mathbf{k} \text{Re}(P_{\mathbf{k}} R_{\mathbf{k}}^*). \quad (2)$$

In homogeneous centrosymmetric media we can expect only a photocurrent proportional to the photon momentum κ . The first term in Eq. (2) represents the drag photocurrent⁴⁻⁶ due to the small (compared with κ) difference between P_k and P_{-k} . The second term vanishes because $|V_k| = |V_{-k}|$. The third—interference—term is associated with the odd part of $\text{Re}(P_k R_k^*)$: it is resonant and proportional to $1/\Delta$. Therefore, the resonant contribution to the photocurrent j_r is of the form $j_r = j - j_{ph} \propto \kappa / \Delta$. Its order of magnitude may be greater or smaller than the background

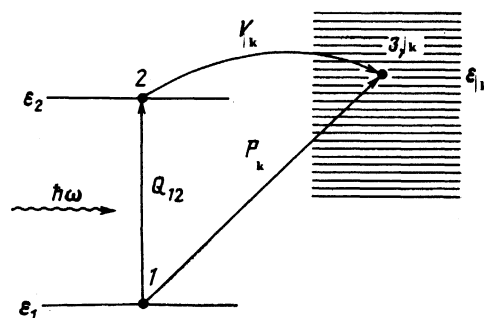


FIG. 1. Schematic representation of resonant absorption of light in a system with a level which interacts with states in the continuous spectrum.

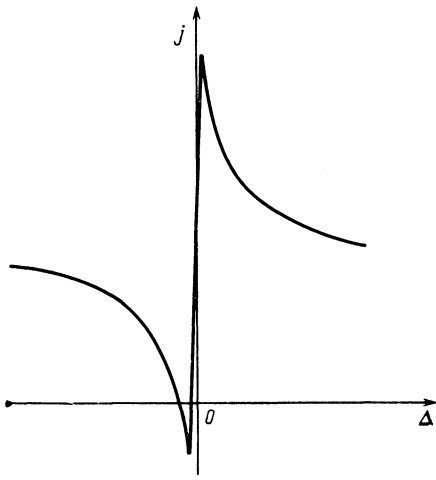


FIG. 2. Typical spectral dependence of a quantum-interference resonant photocurrent.

contribution j_{ph} . A typical dependence $j(\Delta)$ is plotted in Fig. 2.

We must stress an important distinguishing feature of this quantum-interference photocurrent. The ordinary drag current is related to the absorption coefficient by $j \propto d\alpha/d\omega$ (Appendix 1). This applies to resonant⁷⁻⁹ and nonresonant⁴⁻⁶ photocurrents. However, it is clear that the interference photocurrent does not satisfy this relationship. In particular, if $\text{Re}(P_k R_k^*)$ is odd relative to k , the absorption resonance will be Lorentzian, because $j_r \propto 1/\Delta$.

In noncentrosymmetric media in addition to the photocurrent proportional to κ we can expect—as is well known—a photocurrent whose magnitude and direction are governed by the internal asymmetry of the crystal (this is known as the photogalvanic current—see Ref. 10). The presence of an energy level interacting with states in the continuous spectrum may then give rise to a quantum-interference photocurrent whose direction is governed not by the photon wave vector, but by the asymmetry mentioned above. This photocurrent is also related to the part of $\text{Re}(P_k R_k^*)$ odd in κ . It is not proportional to α and obeys the characteristic dispersion law $j_r \propto 1/\Delta$.

It therefore follows that in general a quantum-interference resonant photocurrent consists of two components. One of them is proportional to the photon momentum κ and the other exists only in media without a center of inversion and its direction is a function of the orientation of a crystal.

We now describe an experiment in which a quantum-interference resonant photocurrent was observed.

PHOTOCURRENTS DUE TO OPTICAL TRANSITIONS ACCOMPANIED BY SPIN FLIP IN *n*-TYPE InSb: EXPERIMENT

Until now the optical transitions accompanied by spin flip in *n*-type InSb have been observed in the absorption and photoconductivity spectra.¹¹⁻¹³ The experiments have been carried out in strong magnetic fields, $H \approx 40$ –60 kOe. Two relatively weak peaks separated from one another by ≈ 0.5 kOe have been observed. Both peaks have the Lorentzian profile with a half-width of the order of 0.05 kOe. It has been established that one of the peaks is due to a resonance of electrons bound to impurities (impurity spin resonance ISR) and the other is due to a resonance of free electrons

(spin resonance SR). The difference between the resonance fields arises because the value of the *g* factor of free electrons is somewhat less than that of bound electrons.¹³

In our experiments we investigated the photocurrent in the region of a spin resonance in fields $H = 55$ –57 kOe. A submillimeter NH_3 laser pumped optically by a CO_2 laser (details of the laser used were given in Ref. 14) was employed as the source of the exciting radiation. The submillimeter laser generated single pulses which were nearly triangular with halfwidth 40 ns and a maximum power of ~ 100 kW. The laser radiation wavelength was $90.55 \mu\text{m}$ ($\hbar\omega = 13.7$ meV). At the exit from the laser cell this radiation had a weak linear polarization.

In these experiments we used unpolarized light as well as light with linear or circular polarizations. In the former case the radiation was delivered to a sample using a metal light pipe terminating with a light-concentrating cone. Multiple reflections from the walls of the light pipe and the cone made the transmitted radiation unpolarized. Light with linear polarization was generated by placing a metal grid beyond a laser cell. This linear polarization was converted into circular by a quarter-wave plate made of crystalline quartz. Such polarized light was focused with a long-focus lens. The maximum intensity of light in the sample reached 10 kW/cm^2 . It was lower than the calibrated polyethylene attenuators.

The experiments were carried out in the Faraday geometry, i.e., the direction of light coincided with the magnetic

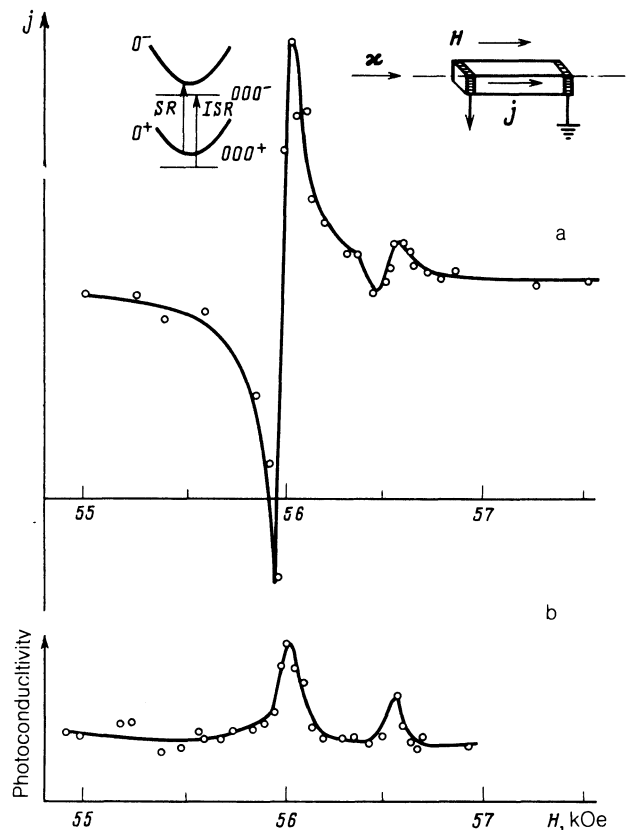


FIG. 3. Dependence of the photocurrent (a) and of the photoconductivity (b) on the applied magnetic field, obtained for sample No. 1 using unpolarized light. The insets show the optical transitions for the impurity spin resonance (ISR) and the spin resonance (SR), as well as the experimental geometry.

TABLE I.

Sample No.	Electron density at $T = 77 \text{ K}$, cm^{-3}	Electron mobility at $T = 77 \text{ K}$, $\text{cm}^2 \cdot \text{V}^{-1} \cdot \text{s}^{-1}$	Orientation of longitudinal axis
1	$6 \cdot 10^{13}$	$7 \cdot 10^5$	unoriented
2	$6 \cdot 10^{13}$	$7 \cdot 10^5$	[100]
3	$6 \cdot 10^{13}$	$7 \cdot 10^5$	[111]
4	$4.5 \cdot 10^{14}$	$4.3 \cdot 10^5$	[100]
5	$4.5 \cdot 10^{14}$	$4.3 \cdot 10^5$	[111]

field. The samples were parallelepipeds with dimensions $3 \times 3 \times 10 \text{ mm}$ and were placed inside the cavity of a superconducting solenoid immersed in liquid helium at $T = 2 \text{ K}$. Ring-shaped ohmic contacts (inset at the top right of Fig. 3) were soldered near the end faces. The orientation of a sample was determined by the light figure method.¹⁵ The properties of the investigated samples are listed in Table I.

In these experiments we determined the magnetic field dependence of the photocurrent longitudinal in relation to the incident light. In some cases we also determined the photoconductivity of a sample. When the field became equal to the value corresponding to the ISR or SR, giant bipolar resonances of the photocurrent were observed and their amplitudes depended on the ratio of the densities of free and bound electrons. For example, in the case of sample No. 1 with a relatively low electron density the ISR of the photocurrent was several times stronger than the SR (Fig. 3a). In the case of samples with a high electron density the opposite was true (Fig. 4).

The very appearance of the photocurrent due to transitions between two localized states of electrons was so unexpected that in order to ensure a more reliable identification

of the resonances, we carried out an additional experiment on the photoconductivity of our samples (Fig. 3b). The positions of the photocurrent resonances on the magnetic field scale coincided with the positions of the photoconductivity resonances which, as pointed out already, corresponded to the ISR and SR.

It is worth noting a number of interesting features of the observed resonances.

1. The absolute value of the resonant photocurrent may exceed the background although the corresponding optical transition is almost forbidden.

2. The direction of the photocurrent is reversed at the resonance point and the transition from the minimum to the maximum value of the photocurrent occurs within the width of the corresponding optical transition.

3. The "wings" of the resonance curves decrease pro-

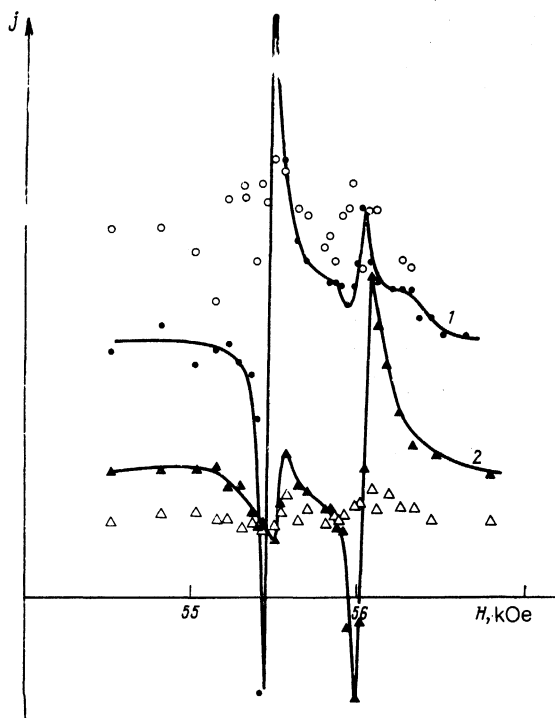


FIG. 4. Dependence of the photocurrent on the magnetic field, obtained for samples Nos. 2 (curve 1, ○ corresponds to the active polarization of light and ● corresponds to the inactive polarization) and 4 (curve 2, △ corresponds to the active polarization, and ▲ corresponds to the inactive polarization).

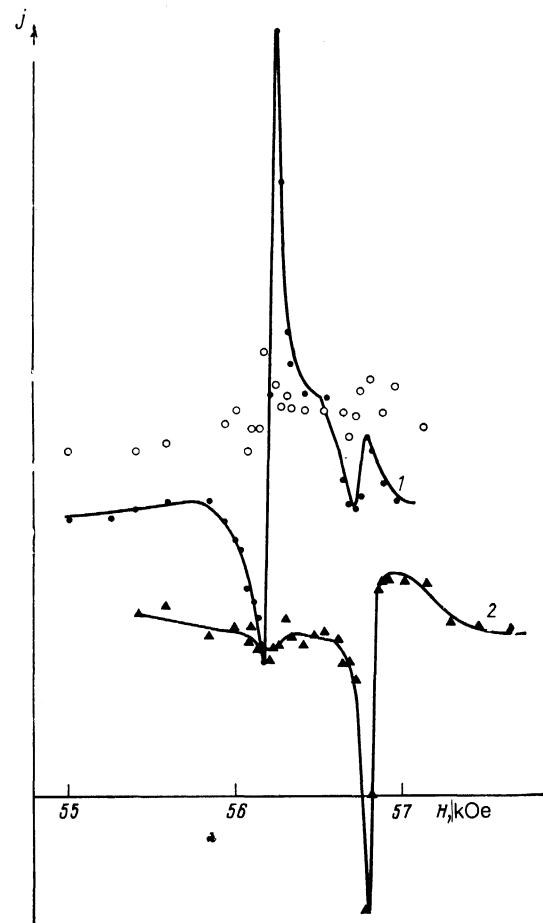


FIG. 5. Dependence of the photocurrent on the magnetic field obtained for sample No. 3 (curve 1, ○ corresponds to the active polarization of light and ● to the inactive polarization) and sample No. 5 (curve 2, inactive polarization). The small differences between the resonance fields for samples Nos. 2, 4 and 3, 5 is due to the anisotropy of the g factor of InSb.¹⁸

portionally to $1/\delta H$ as a function of the offset from resonance, whereas the corresponding absorption profiles are Lorentzian and proportional to $1/(\delta H)^2$, where $\delta H = H - H_r$ and H_r is the resonance magnetic field.

A more detailed investigation of the effect was carried out by measurements employing linearly and circularly polarized light incident on samples oriented along the [100] and [111] directions, and also experiments involving reversal of the directions \mathbf{H} and κ . The dependence obtained in this way is shown in Figs. 4 and 5. It is clear that the resonances of the photocurrent appear only in the cases of linear and cyclotron-inactive circular polarizations of light, and have mainly the same characteristic features as those exhibited by the unpolarized light case, and the effect is¹⁾ even in \mathbf{H} and odd in κ . As reported above, the resonances were observed only when a reversal of the direction of \mathbf{H} or κ was accompanied by a reversal of the sign of the polarization. It was moreover established that the effect was linear in the intensity throughout the investigated range (up to $I \sim 1 \text{ kW/cm}^2$).

QUALITATIVE EXPLANATION OF THE EFFECT

It is known that the spin splitting ϵ_s of the ground Landau level in n -type InSb represents approximately one-third of the cyclotron energy $\hbar\omega_c$ because of the anomalously large value of the g factor ($g = -50$) and in a field of $H = 56 \text{ kOe}$ it amounts to 13.7 meV . Then, since we have $g < 0$, the 0^+ level with the spin $s = 1/2$ lies below the 0^- level with $s = -1/2$. The electron states in the 0^+ and 0^- subbands are classified in accordance with the value of the momentum k along the magnetic field and in accordance with the projection of the orbital momentum m along this direction. In the case of the zeroth Landau band, we have $m = 0, -1, -2, \dots$

The levels of an electron bound to a charged impurity also exhibit the Landau and Zeeman splitting in a magnetic field. Consequently, near the bottom of each free-electron subband there is a series of Coulomb levels which are usually denoted by the symbol $(nm\lambda)^\pm$. Here, n is the Landau level number; m is the projection of the orbital momentum along the magnetic field, which assumes the values $m \leq n$; λ is the quantum number labeling the various impurity states with identical values of m and n , whereas the plus and minus signs correspond to $s = 1/2$ and $s = -1/2$. We are interested in transitions within the lowest ($n = 0$) Landau level.

The experimentally observed impurity resonance is due to a transition from the ground level 000^+ to the level 000^- , which differs from the ground level only by the spin orientation. The free-electron resonance corresponds to the $0^+ \rightarrow 0^-$ transition. We recall that the small difference between the resonance fields of these transitions is due to the difference between the g factors of the bound and free electrons.

We shall now account for the experimental results. We begin with an impurity resonance. Outside the resonance the photocurrent appears because of electric-dipole transitions of electrons from the 000^+ level to the states in the 0^+ band with the momenta k and $-k$ and with the orbital momentum projection along the magnetic field amounting to $m = -1$. This last circumstance arises because in the case of passive polarization of light the photon momentum is -1 , whereas the momentum of an electron in its initial

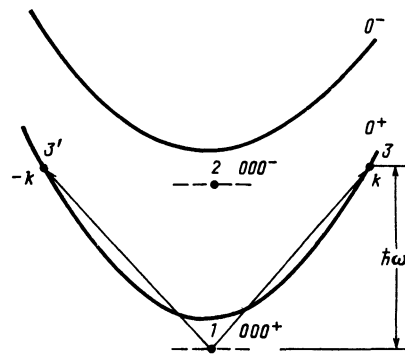


FIG. 6. Schematic representation of the optical transitions from the 000^+ level outside the spin resonance region.

000^+ state is zero. These transitions are identified by arrows in Fig. 6 and these begin from the level 1 and terminate at the levels 3 and $3'$. If we denote the amplitude of the $1 \rightarrow 3$ transition by P_k and that of the $1 \rightarrow 3'$ transition by P_{-k} , we find that the background photocurrent is described by (see the Introduction)

$$j_{\text{ph}} \propto k(P_k^2 - P_{-k}^2) \approx 4\kappa k P_k dP_k/dk. \quad (3)$$

In the region of a resonance (Fig. 7a) we can expect also the composite transitions $1 \rightarrow 2 \rightarrow 3$ and $1 \rightarrow 2 \rightarrow 3'$ via the intermediate state terminating at the level 000^- , of which the $1 \rightarrow 2$ transition is of the magnetic-dipole type, whereas the transitions $2 \rightarrow 3$ and $2 \rightarrow 3'$ occur because of the spin-orbit interaction in the field of the impurity. The final states of the electron in the band are identical with the final states of the transitions $1 \rightarrow 3$ and $1 \rightarrow 3'$, i.e., they also correspond to the projection of the orbital momentum $m = -1$. In fact, the electron orbital momentum at the 000^- level is zero and the spin momentum is $s = -1/2$; the total electron momentum is conserved in the spin-orbit transition to the 0^+ band, where $s = 1/2$, so that in the final state we have $m = -1$.

We denote the amplitudes of the $1 \rightarrow 2 \rightarrow 3$ and $1 \rightarrow 2 \rightarrow 3'$

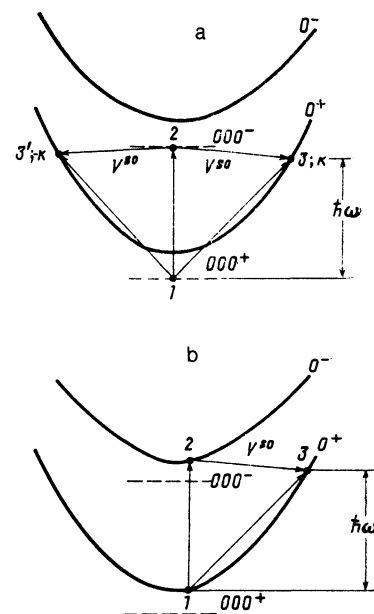


FIG. 7. Schematic representation of transitions from the 000^+ level in the regions of the impurity spin (a) and band-band spin (b) resonances.

transitions by R_k and R_{-k} . Since the spin-orbit interaction is odd in the electron momentum, the value of R_{-k} differs from R_k only in the sign, i.e., $R_{-k} = -R_k$. The total amplitude M_k of the transition from the level 1 to the level 3 is equal to the sum of the amplitudes P_k and R_k : $M_k = P_k + R_k$. We similarly find $M_{-k} = R_{-k} + P_{-k} = P_{-k} - R_k$. The total photocurrent is proportional to the difference between the squares of M_k and M_{-k} :

$$j \propto k(P_k + R_k)^2 - k(P_{-k} - R_k)^2 \approx 4\kappa k \frac{dP_k}{dk} P_k + 4kP_k R_k. \quad (4)$$

The amplitude R_k is equal to the ratio of the product of the matrix elements of the transitions $1 \rightarrow 2$ and $2 \rightarrow 3$ to the difference between the energies Δ of the final 3 and intermediate 2 states. Since the matrix element of the magnetic-dipole transition $1 \rightarrow 2$ is proportional to the photon momentum κ and the quantity Δ is proportional to δH , we find $R_k \propto \kappa/\delta H$. Consequently, the resonant contribution j_r to the photocurrent is given by

$$j_r \propto 4kP_k R_k \propto \kappa/\delta H, \quad (5)$$

which is confirmed by the experimental results.

In the case of active polarization of light the optical transition from the 000^+ level to the 0^+ band is impossible. In fact, in this case the photon momentum is unity, whereas the electron momentum in the 000^+ state is zero and its momentum in the band can only assume values $m \leq 0$, as pointed out already. This accounts for the absence of a resonance in experiments involving active polarization.

The mechanism responsible for the photocurrent in the case of a band-band resonance is similar to that described above (Fig. 7b). The nonresonant contribution is associated with an electric-dipole transition within the 0^+ band ($1 \rightarrow 3$), which is accompanied by the Coulomb scattering of an electron by an impurity. In the resonance region it experiences interference of the composite transition $1 \rightarrow 2 \rightarrow 3$. The $1 \rightarrow 2$ optical transition is of the magnetic-dipole nature, whereas the $2 \rightarrow 3$ transition occurs because of the spin-orbit scattering of an electron in the field of the same impurity, which is active in the $1 \rightarrow 3$ electric-dipole transition. The contributions of the $1 \rightarrow 3$ and $1 \rightarrow 2 \rightarrow 3$ transitions, due to the scattering by different impurities, vanishes after averaging over the impurity positions.

We conclude this section by noting that optical transitions accompanied by spin flip may also be due to the k^3 terms in the Hamiltonian (known as the combined resonance—see Refs. 17 and 18). It is this process that makes the principal contribution to the $1 \rightarrow 2$ absorption, since—according to Ref. 18—its probability is much higher than the probability of the magnetic-dipole transition. However, using the results of Ref. 18 we can show that in the Faraday geometry the $1 \rightarrow 2 \rightarrow 3$ composite transition involving a contribution of the k^3 terms does not interfere with the $1 \rightarrow 3$ electric-dipole transition, because their amplitudes differ in phase by $\pi/2$.

ANALYTIC THEORY

1. Impurity resonance

It follows from a qualitative analysis that in the case under discussion the important interaction is that between

the state at the 000^- level and the states in the 0^+ subband with the orbital momentum projection along the magnetic field direction (z axis) amounting to -1 . The corresponding wave functions will be denoted by $\chi_0(\mathbf{r})$ and $\varphi_k(\mathbf{r})$. We shall ignore the nonparabolicity of the 0^+ subband and assume that $\varepsilon_k = k^2/2m$. The function $\varphi_k(\mathbf{r})$ allows for the Coulomb scattering of an electron on an impurity. We adopt the following normalization conditions:²⁾

$$\int |\chi_0(\mathbf{r})|^2 d\mathbf{r} = 1, \quad \int \varphi_k^*(\mathbf{r}) \varphi_{k'}(\mathbf{r}) d\mathbf{r} = \delta(k-k'),$$

$$\int \varphi_k^*(\mathbf{r}) \chi_0(\mathbf{r}) d\mathbf{r} = 0. \quad (6)$$

The functions χ_0 and φ_k are the eigenfunctions of the Hamiltonian \mathcal{H}_0 , which does not include the interaction V between the level and the band. In the case of this interaction we assume that only the matrix elements of the $\int \varphi_k^*(\mathbf{r}) V(\mathbf{r}) \chi_0(\mathbf{r}) d\mathbf{r} = V_{k0}$ type do not vanish, since $V_{00} = V_{kk} = 0$.

We now have to find the eigenfunctions Φ_k of the Hamiltonian $\mathcal{H}_0 + V$, such that $\Phi_k \rightarrow \varphi_k$ in the limit $V \rightarrow 0$. This is the familiar Fano problem.³ We outline the solution of this problem.

The function Φ_k satisfies an integral equation

$$\Phi_k^\pm(\mathbf{r}) = \varphi_k^\pm(\mathbf{r}) + \int G^\pm(\mathbf{r}, \mathbf{r}') V(\mathbf{r}') \Phi_k^\pm(\mathbf{r}') d\mathbf{r}', \quad (7)$$

where $G_k^\pm(\mathbf{r}, \mathbf{r}')$ is the Green's function of the operator \mathcal{H}_0 :

$$G_k^\pm(\mathbf{r}, \mathbf{r}') = \frac{\chi_0(\mathbf{r}) \chi_0^*(\mathbf{r}')}{\varepsilon_k - \varepsilon_0} + \int_{-\infty}^{+\infty} \frac{\varphi_{k'}^\pm(\mathbf{r}) \varphi_{k'}^{\pm*}(\mathbf{r}') dk'}{\varepsilon_k - \varepsilon_{k'} \pm i\gamma}, \quad \gamma \rightarrow 0, \quad (8)$$

ε_0 is the energy of the discrete level, whereas the plus and minus signs correspond to the diverging and converging waves, respectively. We seek the solution of the above equation in the form

$$\Phi_k^\pm(\mathbf{r}) = \alpha_0^\pm(k) \chi_0(\mathbf{r}) + \int_{-\infty}^{+\infty} \alpha_{k'}^\pm(k) \varphi_{k'}^\pm(\mathbf{r}) dk'. \quad (9)$$

Substituting Eqs. (8) and (9) into Eq. (7), we obtain a system of equations

$$\alpha_0^\pm(k) = \frac{1}{\varepsilon_k - \varepsilon_0} \int_{-\infty}^{+\infty} \alpha_{k'}^\pm(k) V_{0k'} dk',$$

$$\alpha_{k'}^\pm(k) = \delta(k-k') + \alpha_0^\pm(k) \frac{V_{k'0}}{\varepsilon_k - \varepsilon_{k'} \pm i\gamma}, \quad (10)$$

from which we find that

$$\alpha_0^\pm(k) = V_{0k} \left(\varepsilon_k - \varepsilon_0 - \int_{-\infty}^{+\infty} \frac{|V_{0k'}|^2}{\varepsilon_k - \varepsilon_{k'} \pm i\gamma} dk' \right)^{-1},$$

$$\alpha_{k'}^\pm(k) = \delta(k-k') + \frac{V_{0k} V_{k'0}}{\varepsilon_k - \varepsilon_{k'} \pm i\gamma} \left(\varepsilon_k - \varepsilon_0 - \int_{-\infty}^{+\infty} \frac{|V_{0k'}|^2}{\varepsilon_k - \varepsilon_{k'} \pm i\gamma} dk' \right)^{-1} \quad (11)$$

Below we will need the probability of a transition to the state Φ_k . In calculating this probability it is necessary to use the function $\Phi_k^-(\mathbf{r})$. We obtain an expression for this function by substituting Eq. (11) into Eq. (9):

$$\Phi_{k^-}(\mathbf{r}) = \varphi_{k^-}(\mathbf{r}) + \frac{V_{0k}\chi_0(\mathbf{r})}{\varepsilon_k - \varepsilon_0 - \delta_0(k) - i\Gamma(k)} + \frac{V_{0k}}{\varepsilon_k - \varepsilon_0 - \delta_0(k) - i\Gamma(k)} \int_{-\infty}^{+\infty} \frac{\varphi_{k'}^-(\mathbf{r}) V_{k'0}}{\varepsilon_k - \varepsilon_{k'} - i\gamma} dk', \quad (12)$$

where

$$\delta_0(k) = \int_{-\infty}^{+\infty} \frac{|V_{0k'}|^2}{\varepsilon_k - \varepsilon_{k'}} dk', \quad \Gamma(k) = 2\pi \frac{m}{k} |V_{0k}|^2.$$

The second term in Eq. (12) is the contribution of the wave function of a discrete level to the exact wave function of the continuous spectrum, whereas the third describes the resonant scattering of an electron by a level because of the interaction V . Both these terms are small compared with the first value of ε_k , with the exception of the region of the resonance where $|\varepsilon_k - \varepsilon_0 - \delta_0(k)| \sim \Gamma(k)$. The quantity $\delta_0(k)$ is a small shift of the level due to the interaction, whereas $\Gamma(k)$ is the resonance half-width.

In fact, the wave functions of an electron at the level in question and in the band are spinors with the "down" spin ($s = -1/2$) and the "up" spin ($s = 1/2$), respectively. We denote these spinors by $\hat{\chi}_{0i}$ and $\hat{\varphi}_{k\pm}$:

$$\hat{\chi}_{0i} = \begin{pmatrix} 0 \\ 1 \end{pmatrix} \chi_{0i}(\mathbf{r}), \quad \hat{\varphi}_{k\pm} = \begin{pmatrix} 1 \\ 0 \end{pmatrix} \varphi_{k\pm}(\mathbf{r}). \quad (13)$$

Then, the exact wave function $\hat{\Phi}_{k^-}$ is described by

$$\hat{\Phi}_{k^-}(\mathbf{r}) = \hat{\varphi}_{k\pm}^-(\mathbf{r}) + \frac{\hat{\chi}_{0i}(\mathbf{r}) V_{0i,k\pm}}{\varepsilon_k - \varepsilon_- - i\Gamma(k)} + \frac{V_{0i,k\pm}}{\varepsilon_k - \varepsilon_- - i\Gamma(k)} \int_{-\infty}^{+\infty} \frac{\hat{\varphi}_{k'\pm}^-(\mathbf{r}) V_{k'\pm,0}}{\varepsilon_k - \varepsilon_{k'} - i\gamma} dk', \quad (14)$$

where ε_- is the energy of an electron at the 000^- level and V^{so} is the spin-orbit interaction operator, which in the case of InSb can be written in the form¹⁹

$$V^{so} = -\frac{\alpha}{\hbar} \left(\sigma \left[\nabla V \times \left(-i\hbar \nabla + \frac{e}{c} \mathbf{A}_0 \right) \right] \right) = -\frac{\alpha}{\hbar} (\sigma \left[\nabla V \times \hat{\mathbf{k}} \right]), \quad (15)$$

$$\alpha = \frac{\hbar^2 \Delta (2E_g + \Delta) E_p}{6m_0 (E_g + \Delta)^2 E_g^2}, \quad E_p = \frac{2p^2}{m_0}.$$

Here, $V = -e^2/\varepsilon r$ is the Coulomb energy of the interaction of an electron with an impurity; $\hat{\mathbf{k}}$ is the kinematic momentum operator; ε is the permittivity; σ_x , σ_y , and σ_z are the Pauli matrices; $\mathbf{A}_0 = 1/2[\mathbf{H} \times \mathbf{r}]$ is the vector potential of the magnetic field; p is the interband matrix element of the momentum; m_0 is the mass of a free electron; Δ is the spin-orbit splitting of the valence band; E_g is the width of the band gap; $(\dots \times \dots)$ and denotes a vector product; and $[\dots, \dots]$ is a commutator.

It is convenient to rewrite the operator V^{so} in the form

$$V^{so} = (2^{1/2} \alpha / \hbar^2) \{ \sigma_- ([\hat{k}_z, V] \hat{k}_+ - [\hat{k}_+, V] \hat{k}_z) + \sigma_+ ([\hat{k}_-, V] \hat{k}_- - [\hat{k}_-, V] \hat{k}_+) \}, \quad (16)$$

where

$$\sigma_{\pm} = 1/2 (\sigma_x \pm i\sigma_y), \quad \hat{k}_{\pm} = 2^{-1/2} (\hat{k}_x \pm i\hat{k}_y).$$

The operator of the interaction of an electron with an electromagnetic field of the optical wave is \mathcal{H}' and it is described by

$$\mathcal{H}' = \mathcal{H}_1 + \mathcal{H}_2 = \frac{e}{mc} (\mathbf{A}_\gamma \hat{\mathbf{k}}) + \frac{g\mu_B}{2} (\mathbf{H}_\gamma \boldsymbol{\sigma}), \quad (17)$$

where \mathbf{A}_γ is the vector potential of the electromagnetic fields; μ_B is the Bohr magneton; m is the effective mass of an electron in InSb; and $\mathbf{H}_\gamma = \text{curl} \mathbf{A}_\gamma$ is the magnetic field of the optical wave. The first term \mathcal{H}_1 in Eq. (17) is responsible for the electric-dipole transition of an electron from the 000^+ level to the 0^+ band and the second term \mathcal{H}_2 is responsible for the magnetic-dipole transition to the 000^- level.

The wave functions $\hat{\chi}_{0i}$ and $\hat{\chi}_{0v}$ of an electron at the levels 000^+ and 000^- , considered in the adiabatic approximation, can be written in the form²⁰

$$\hat{\chi}_{0i} = \begin{pmatrix} 1 \\ 0 \end{pmatrix} \chi_{0i}(\mathbf{r}), \quad \hat{\chi}_{0v} = \begin{pmatrix} 0 \\ 1 \end{pmatrix} \chi_{0v}(\mathbf{r}), \quad (18)$$

$$\chi_{0i}(\mathbf{r}) = \frac{2^{-1/2}}{a_H} \left(\frac{\kappa_0}{2\pi} \right)^{1/2} \exp \left(-\frac{\rho^2}{4a_H^2} - \kappa_0 |z| \right),$$

and the wave function $\hat{\varphi}_{k\pm}$ for the 0^+ band, corresponding to the orbital momentum $m = -1$, is

$$\hat{\varphi}_k = \frac{1}{(2\pi\hbar)^{1/2}} \exp \left(\frac{ikz}{\hbar} \right) \frac{1}{(2\pi)^{1/2}} \times \exp(-i\varphi) \frac{\rho}{2^{1/2} a_H^2} \exp \left(-\frac{\rho^2}{4a_H^2} \right) \begin{pmatrix} 1 \\ 0 \end{pmatrix}. \quad (19)$$

Here, $\alpha_H = (\hbar c/eH)^{1/2}$ is the magnetic length, $\rho^2 = x^2 + y^2$, φ is the polar angle, $\kappa_0 = (a_B v_0)^{-1}$, $v_0 = 1/2 \ln(a_B/a_H)$, and a_B is the Bohr radius. In the expression for $\hat{\varphi}_k$ we ignored the scattering of electrons by the center.

The total amplitude M_k of an electron transition from the 000^+ level to the 0^+ band is equal to the matrix element of the operator \mathcal{H}' calculated using the functions $\hat{\chi}_{0i}$ and $\hat{\Phi}_{k^-}$:

$$M_k = \langle \hat{\Phi}_{k^-} | \mathcal{H}' | \hat{\chi}_{0i} \rangle = \langle \hat{\varphi}_{k\pm}^- | \mathcal{H}_1 | \hat{\chi}_{0i} \rangle + V_{k\pm,0i}^{so} \langle \hat{\chi}_{0i} | \mathcal{H}_2 | \hat{\chi}_{0i} \rangle [\varepsilon_k - \varepsilon_- + i\Gamma(k)]^{-1} + \frac{V_{k\pm,0i}^{so}}{\varepsilon_k - \varepsilon_- + i\Gamma(k)} \int_{-\infty}^{+\infty} \frac{V_{0i,k'\pm} \langle \hat{\varphi}_{k'\pm}^- | \mathcal{H}_1 | \hat{\chi}_{0i} \rangle dk'}{\varepsilon_k - \varepsilon_{k'} + i\gamma}. \quad (20)$$

The first term on the right-hand side of the above equation represents the amplitude P_k of the $1 \rightarrow 3$ electric-dipole transition, whereas the second is the amplitude R_k of the $1 \rightarrow 2 \rightarrow 3$ composite transition. The third term is the amplitude of the electric-dipole transition to the 0^+ band accompanied by simultaneous resonance scattering of an electron at the 000^- level.

The vector potentials corresponding to the active (plus sign) and passive (minus sign) polarizations of light are given by

$$\mathbf{A}_\gamma^\pm = \frac{A_\gamma}{2^{1/2}} (\mathbf{e}_x \pm i\mathbf{e}_y) \exp \left(\frac{i\kappa z}{\hbar} \right),$$

where \mathbf{e}_x and \mathbf{e}_y are unit vectors along the x and y axes. Consequently, the Hamiltonian \mathcal{H}' is described by

$$\mathcal{H}'^\pm = \mathcal{H}_1^\pm + \mathcal{H}_2^\pm = \frac{eA_\gamma}{mc} \exp \left(\frac{i\kappa z}{\hbar} \right) \hat{k}_\pm + \frac{\kappa |g| \mu_B A_\gamma}{2^{1/2} \hbar} \exp \left(\frac{i\kappa z}{\hbar} \right) \sigma_\pm. \quad (21)$$

Therefore, in the inactive polarization case, we obtain

$$P_k = \frac{eA_T}{mc} \int d\mathbf{r} \varphi_k^*(\mathbf{r}) \exp\left(\frac{i\kappa z}{\hbar}\right) \hat{k}_- \chi_0(\mathbf{r}).$$

It is not possible to find directly the value of the integral using the function $\chi_0(\mathbf{r})$ in the adiabatic approximation of Eq. (18), because in this approximation we have $\hat{k}_- \chi_0(\mathbf{r}) = 0$. A method which makes it possible to bypass this difficulty is suggested in Appendix 2. In the approximation which is linear in κ , we obtain

$$P_k = i \frac{2^{1/2} e \omega \hbar^2 a_H \kappa_0 A_T}{c \hbar^2} \left(\frac{\kappa_0}{2\pi \hbar}\right)^{1/2} \left(1 + \frac{\kappa}{k} \frac{2\omega}{2\omega + \omega_c}\right),$$

where $\omega_c = eH/mc$ is the cyclotron frequency. If the matrix element is described by $V_{k_1, 0_1}^{s_0}$ and Eqs. (16), (18), and (19) are applied, and if we assume $\hbar \kappa_0 \ll k$, the result is

$$V_{k_1, 0_1}^{s_0} = -i \frac{\kappa_0^{1/2} \alpha e^2 k}{4e \hbar^{3/2}} \left\{ 1 - \left(\frac{\pi \omega}{\omega_c}\right)^{1/2} \exp\left(\frac{\omega}{\omega_c}\right) \operatorname{erf}\left[\left(\frac{\omega}{\omega_c}\right)^{1/2}\right] \right\} \quad (22)$$

The expression in the braces is approximately equal to 0.4 under the conditions in our experiments. Now, using Eq. (22) and the expression in Eq. (21) for the operator \mathcal{H}_2^- , we obtain the amplitude of the composite 1 → 2 → 3 transition:

$$R_k = -i \kappa \frac{0.4 A_T |g| \alpha e^2 \kappa_0^{1/2} \mu_B k}{2^{1/2} e \hbar^{3/2}} \frac{1}{\Delta + i\Gamma(k)},$$

$$\Delta = \varepsilon_k - \varepsilon_- = \hbar \omega - (\varepsilon_- - \varepsilon_+),$$

where ε_+ is the energy of an electron at the 000⁺ level.

The contribution of the third term in Eq. (20) to the total transition amplitude is relatively small and we shall ignore it.

We describe the photocurrent by the expression

$$j = e \frac{2\pi}{\hbar} (|M_k|^2 - |M_{-k}|^2) \frac{\langle k \rangle}{m} \rho(\varepsilon_k) \tau_k n_{im}, \quad (23)$$

where $\rho(\varepsilon_k) = m/k$ is the density of the final states, τ_k is the momentum relaxation time, n_{im} is the electron density at impurities, and $\langle k \rangle$ is the average value of the momentum which is not equal to k because of the resonant scattering by the investigated level:

$$\langle k \rangle = k \Delta^2 / [\Delta^2 + \Gamma^2(k)].$$

In our case the momentum relaxation process is mainly due to the scattering by charged impurities whose concentration is N , so that the value of τ_k is described by²¹

$$\tau_k^{-1} = \frac{8\pi}{2^{1/2}} \frac{\varepsilon_B}{\hbar} N a_H^3 \left(\frac{\hbar \omega_c}{\varepsilon_k}\right)^{1/2} \Phi_0\left(\frac{\omega}{\omega_c}\right),$$

where ε_B is the Bohr energy and the function $\Phi_0(\omega/\omega_c)$ is approximately equal to 0.25 at $\omega_c \approx 3\omega$. Therefore, bearing in mind that $M_k = P_k + R_k$ and substituting the expressions for P_k , R_k , $\langle k \rangle$, and τ_k into Eq. (23), we obtain

$$j = j_{ph} \left(1 + \frac{H_1 \cdot \delta H}{(\delta H)^2 + \tilde{\gamma}^2}\right) \frac{(\delta H)^2}{(\delta H)^2 + \tilde{\gamma}^2}, \quad (24)$$

where

$$\tilde{\gamma} = \frac{\Gamma}{|g| \mu_B},$$

$$j_{ph} = e \frac{\kappa}{m} |n_{im}| \frac{1}{\pi} \left(\frac{2eEa_H}{\hbar \omega}\right)^2 \frac{|e_+|}{|\varepsilon_B|} \frac{\omega}{2\omega + \omega_c} \frac{\kappa_0}{N a_H^2},$$

$$H_1 \cdot = \left(\frac{\pi}{2}\right)^{1/2} \frac{0.4 e m^2 c (2\hbar \omega + \hbar \omega_c) \Delta (2E_g + \Delta) E_p}{12 e a_H m_0 \hbar E_g^2 (E_g + \Delta)^2}.$$

Here, $E = \omega A_T/c$ is the electric field of an optical wave.

Since under our experimental conditions we have $|e_+|/|\varepsilon_B| \approx 3$, we can use the known properties of InSb and thus obtain the final expression for the photocurrent j :

$$j = e \frac{\kappa}{m} |n_{im}| \frac{10^{15} [\text{cm}^{-3}]}{N [\text{cm}^{-3}]} \frac{I}{I_1} \left(1 + \frac{H_1 \cdot \delta H}{(\delta H)^2 + \tilde{\gamma}^2}\right) \frac{(\delta H)^2}{(\delta H)^2 + \tilde{\gamma}^2}, \quad (25)$$

where I is the intensity of light inside the investigated crystal, $I_1^* = 5 \times 10^5 \text{ W/cm}^2$, and $H_1^* = 30 \text{ Oe}$.

2. Band-band resonance

Calibration of the vector potential of a static magnetic field can now be selected conveniently in the form

$$A_x = -Hy, \quad A_y = A_z = 0.$$

Then, the coordinate part of the wave function of a free electron can be written as follows:¹⁹

$$\psi_{nkq}(x, y, z) = \frac{1}{L} \exp\left[\frac{i}{\hbar}(kz + qx)\right] \chi_{nq}(y),$$

$$\chi_{nq}(y) = [\pi^{1/2} a_H^{-1/2} (2^n n!)^{-1/2}]^{-1} \exp\left[-\frac{(y-y_q)^2}{2a_H^2}\right] H_n\left(\frac{y-y_q}{a_H}\right),$$

$$y_q = cq/eH = a_H^2 q/\hbar,$$

where n is the Landau level number, q is the momentum of an electron along the x axis governing the position of an oscillator y_q on the y axis, L is the size of the investigated crystal, and H_n is a Hermite polynomial.

The complete wave function $\hat{\psi}_{nkq}$ which includes the spin variable has the following form for the "up" spin

$$\hat{\psi}_{nkq\uparrow} = \begin{pmatrix} 1 \\ 0 \end{pmatrix} \psi_{nkq},$$

while for the "down" spin, it becomes

$$\hat{\psi}_{nkq\downarrow} = \begin{pmatrix} 0 \\ 1 \end{pmatrix} \psi_{nkq}.$$

The electron energy in the band is

$$\varepsilon_{nk\pm} = (n + 1/2) \hbar \omega_c \mp |g| \mu_B H/2 + k^2/2m_e.$$

The plus and minus signs correspond to the "up" and "down" spins. We denote the spin splitting by ε_s . An operator k_+ acting on the function ψ_{nkq} transforms it into $\psi_{n+1, k, q}$, whereas the operator \hat{k} transforms it into $\psi_{n-1, k, q}$. For example, we find that

$$\hat{k}_+ \psi_{0kq} = -\frac{\hbar}{a_H} \psi_{1kq}, \quad \hat{k}_- \psi_{1kq} = -\frac{\hbar}{a_H} \psi_{0kq}, \quad \hat{k}_- \psi_{0kq} = 0. \quad (26)$$

These properties of the operators \hat{k}_{\pm} as well as the properties of the matrices σ_{\pm} yield the selection rules for the electric- and magnetic-dipole transitions. We identify those which will be required later. The operator \mathcal{H}_1^+ transfers an

electron from the band 0^+ to the band 1^+ , whereas the operator \mathcal{H}_1^- does the reverse: it transfers it from the band 1^+ to the band 0^+ . This means that direct absorption of light because of the electric-dipole interaction is possible only in the active polarization case.

The operator \mathcal{H}_2^+ transfers an electron from the band 0^+ to the band 0^- , whereas the operator \mathcal{H}_2^- transfers it from the band 0^- to the band 0^+ . Therefore, in the InSb case (which is characterized by $g < 0$) we can expect direct absorption because of the magnetic-dipole interaction only for the inactive polarization of light.

In our case the optical transitions are indirect and are accompanied by the scattering of an electron on impurities with a potential V :

$$V = \sum_i \frac{\pm e^2}{\epsilon |\mathbf{r} - \mathbf{r}_i|},$$

where the summation is carried out over the impurity coordinates.

We first consider the inactive polarization of light. It is then sufficient to limit the treatment to the second order of perturbation theory. An electric-dipole transition from the state $\hat{\psi}_{0kq_1}$ to the state $\hat{\psi}_{0k'q'_1}$ (1-3 transition in Fig. 7b) occurs in accordance with the scheme shown in Fig. 8. The Coulomb interaction with an impurity scatters an electron from the state $\hat{\psi}_{0kq_1}$ to the intermediate state $\hat{\psi}_{1k'-\kappa q'_1}$. The amplitude of this transition can be written in the form $\langle \hat{\psi}_{1k'-\kappa q'_1} | V | \hat{\psi}_{0kq_1} \rangle$. Then a photon is absorbed and an electron is transferred to the final state $\hat{\psi}_{0k'r'q'_1}$. The amplitude of this transition is $\langle \hat{\psi}_{0k'r'q'_1} | \mathcal{H}_1^- | \hat{\psi}_{1k'-\kappa q'_1} \rangle$ (when a photon is absorbed, the electron momentum along the z axis changes by κ and its momentum along the x axis is unaffected).

According to the selection rules of perturbation theory, the amplitude $P_{k'}$ of the process of interest to us is described by the expression

$$P_{k'} = \frac{\langle \hat{\psi}_{0k'r'q'_1} | \mathcal{H}_1^- | \hat{\psi}_{1k'-\kappa q'_1} \rangle \langle \hat{\psi}_{1k'-\kappa q'_1} | V | \hat{\psi}_{0kq_1} \rangle}{\epsilon_{k'} - \hbar\omega_c - \hbar\omega - \epsilon_{k'-\kappa}},$$

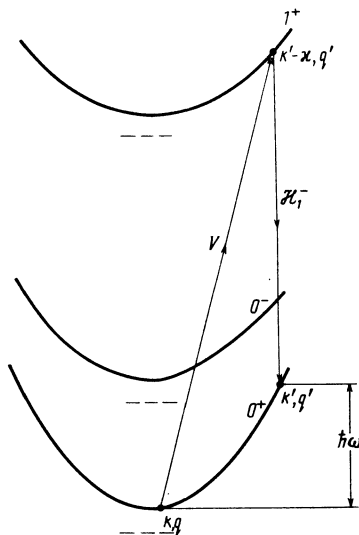


FIG. 8. Schematic representation of an electric-dipole transition of a free electron from a state $\hat{\psi}_{0kq_1}$ to a state $\hat{\psi}_{0k'r'q'_1}$.

where the denominator is equal to the difference between the energies of the final and intermediate states; here, $\epsilon_{k'}$, and $\epsilon_{k'-\kappa}$ represent the kinetic energies of an electron in the bands. For all values of k' the denominator is finite and close to $-\hbar\omega_c - \hbar\omega$. Since

$$\begin{aligned} \mathcal{H}_1^- \hat{\psi}_{1k'-\kappa q'_1} &= -\frac{eA_T \hbar}{mc a_H} \exp\left(\frac{i\kappa z}{\hbar}\right) \hat{\psi}_{0k'-\kappa q'_1} \\ &= -\frac{eA_T \hbar}{mc a_H} \hat{\psi}_{0k'q'_1}, \end{aligned}$$

it follows that the expression for a matrix element of \mathcal{H}_1^- is

$$\langle \hat{\psi}_{0k'q'_1} | \mathcal{H}_1^- | \hat{\psi}_{1k'-\kappa q'_1} \rangle = -eA_T \hbar / mca_H.$$

The Coulomb interaction operator is independent of the spin, so that

$$\begin{aligned} \langle \hat{\psi}_{1k'-\kappa q'_1} | V | \hat{\psi}_{0kq_1} \rangle &= \langle \hat{\psi}_{1k'-\kappa q'_1} | V | \hat{\psi}_{0kq} \rangle \\ &= \int \hat{\psi}_{1k'-\kappa q'_1}^*(\mathbf{r}) V(\mathbf{r}) \hat{\psi}_{0kq}(\mathbf{r}) d\mathbf{r}. \end{aligned}$$

Therefore, the matrix element for an electric-dipole transition can be written in the form

$$P_{k'} = \frac{eA_T \hbar}{mca_H} \frac{\langle \hat{\psi}_{1k'-\kappa q'_1} | V | \hat{\psi}_{0kq} \rangle}{\epsilon_{k'-\kappa} + \hbar\omega_c + \hbar\omega - \epsilon_{k'}}.$$

The composite transition is shown schematically in Fig. 9. The corresponding amplitude $R_{k'}$ is of the form

$$R_{k'} = \frac{\langle \hat{\psi}_{0k'r'q'_1} | V^{so} | \hat{\psi}_{0k+\kappa q_1} \rangle \langle \hat{\psi}_{0k+\kappa q_1} | \mathcal{H}_2^- | \hat{\psi}_{0kq_1} \rangle}{\epsilon_{k'} - \epsilon_{k+\kappa} - \epsilon_s}.$$

The denominator in the above expression exhibits a resonance, so that

$$\epsilon_{k'} - \epsilon_{k+\kappa} - \epsilon_s \approx \epsilon_{k'} - \epsilon_k - \epsilon_s = \hbar\omega - \epsilon_s.$$

The matrix element of \mathcal{H}_2^- is described by

$$\langle \hat{\psi}_{0k+\kappa q_1} | \mathcal{H}_2^- | \hat{\psi}_{0kq_1} \rangle = \kappa |g| \mu_B A_T / 2^{1/2} \hbar.$$

To calculate the matrix element of the operator V^{so} we need to allow only for the second term in Eq. (16), because only this term transfers an electron from the band 0^- to the band 0^+ :

$$\begin{aligned} \langle \hat{\psi}_{0k'r'q'_1} | V^{so} | \hat{\psi}_{0k+\kappa q_1} \rangle &= \frac{2^{1/2} \alpha}{\hbar^2} \langle \hat{\psi}_{0k'r'q'_1} | \sigma_+ ([k_-, V] k_s \\ &- [k_s, V] k_-) | \hat{\psi}_{0k+\kappa q_1} \rangle = \frac{2^{1/2} \alpha (k+\kappa)}{\hbar a_H} \langle \hat{\psi}_{1k'-\kappa q'_1} | V | \hat{\psi}_{0kq} \rangle. \end{aligned}$$

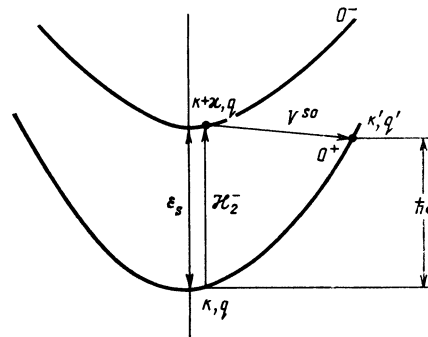


FIG. 9. Schematic representation of the composite transition of a free electron.

In these calculations we used the relationship given in Eq. (26) and the fact that the operator \hat{k}_- is the Hermitian conjugate of the operator \hat{k}_+ . Finally, the expression for $R_{k'}$ becomes

$$R_{k'} = -\kappa \frac{\alpha(k+\kappa) |g| \mu_B A_\gamma}{\hbar^2 a_H} \frac{\langle \psi_{ik'-\kappa q'} | V | \psi_{0kq} \rangle}{\epsilon_{k'-\kappa} - \epsilon_{k+\kappa} - \epsilon_s}.$$

The total amplitude $M_{k'}$ of the transition from a state $\hat{\psi}_{0kq_1}$ to a state $\hat{\psi}_{0k'q'}$ is equal to the sum of the amplitudes $P_{k'}$ and $R_{k'}$:

$$M_{k'} = P_{k'} + R_{k'}.$$

The transition probability is proportional to the square of the absolute value of the transition amplitude:

$$|M_{k'}|^2 = |P_{k'}|^2 + |R_{k'}|^2 + P_{k'} R_{k'}^* + P_{k'}^* R_{k'}.$$

In calculation of the photocurrent it is important to allow for the contribution which is linear in the photon momentum. Such a contribution occurs, firstly, in the expression for $|P_{k'}|^2$ and is related to the background photocurrent which exists outside a resonance. The contribution of a resonance to the photocurrent is represented by an interference term $P_{k'} R_{k'}^* + P_{k'}^* R_{k'}$.

In addition to the transitions shown in Figs. 8 and 9, we have to allow also for transitions to the state $\Psi_{0-k'q'}$, i.e., to a state which differs from $\hat{\psi}_{0-k'q'}$ only by the direction of the momentum k (Fig. 10). We denote the amplitudes of these transitions by $P_{-k'}$ and $R_{-k'}$ and their sum by $M_{-k'}$. The total probabilities $W_{k'}$ and $W_{-k'}$ of the transitions from a state with a momentum k to one with the momenta k' and $-k'$ are proportional to $|M_{k'}|^2$ and $|M_{-k'}|^2$, averaged over the positions of the scattering impurities. Then, as pointed out in the preceding section, the contribution to the interference term made by the $1 \rightarrow 3$ and $1 \rightarrow 2 \rightarrow 3$ transitions, due to the scattering on different impurities, vanishes. The current density is then

$$j = e \int_{-\infty}^{\infty} f(k) \frac{\hbar k'}{m} \tau(k') (W_{k'} - W_{-k'}) dk,$$

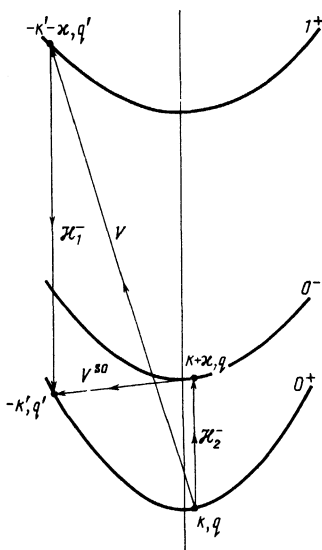


FIG. 10. Transitions of a free electron to states $\hat{\psi}_{0-k'q'}$.

where $f(k)$ is the distribution function of free electrons in the subband 0^+ normalized to the density of free electrons n_{fr} ; $\tau(k')$ is the momentum relaxation time, which—in our case—is determined by the scattering on impurities. Dropping the intermediate calculation stages, we obtain

$$j = 4,6 en_{fr} \frac{\kappa}{m} \left(\frac{2eEa_H}{\hbar\omega} \right)^2 \frac{\omega\omega_s^2}{(\omega+\omega_s)^3} \times \left[1 - \frac{0,9\alpha |g| \mu_B cm^3 kT (\hbar\omega_s + \hbar\omega)^2}{e\hbar^3 (\hbar\omega - \epsilon_s)} \right],$$

where T is the electron temperature. It is interesting to note that the photocurrent is independent of the impurity concentration N . This is because the transition probabilities $W_{k'}$ and $W_{-k'}$ are directly proportional to N , whereas the relaxation time $\tau(k')$ is inversely proportional to the impurity concentration.

Using the parameters of InSb and assuming that the electron temperature is equal to the lattice temperature, we finally obtain

$$j = e \frac{\kappa}{m} n_{fr} \frac{I}{I_2} \left(1 + \frac{H_2^*}{\delta H} \right), \quad (27)$$

$$I_2^* \approx 6,2 \cdot 10^5 \text{ W/cm}^2, \quad H_2^* \approx 15 \text{ Oe}.$$

We now compare the theoretical predictions with experiments. It follows from the above analysis that a quantum-interference resonant photocurrent should exhibit a specific magnetic-field dependence: $j_r \propto 1/\delta H$. Figure 11 shows the experimental dependence of the photocurrent on the applied magnetic field in the case of an impurity resonance alongside a theoretical dependence of the type

$$(j - j_{ph})/j_{ph} = H_1^*/\delta H,$$

deduced from Eq. (24) in the limit $\gamma \ll \delta H$. We can see that the agreement between the experimental points and the calculated curve is good if we assume that $H_1^* = 80 \text{ Oe}$. The experimental value is slightly greater than that found by cal-

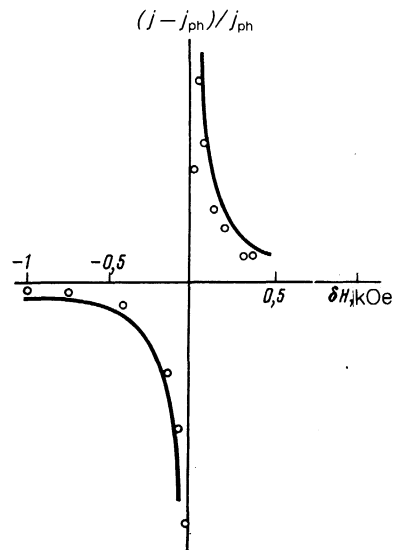


FIG. 11. Dependence of the normalized resonant photocurrent $(j - j_{ph})/j_{ph}$ on the offset δH . The points are the experimental values (sample No. 1). The continuous curve is the dependence (28).

culations possibly because the experimentally determined current also includes the contribution of intraband transitions.

A quantitative comparison carried out for a band—band resonance shows that the dependence

$$\frac{j - j_{ph}}{j_{ph}} = \frac{H_2^*}{\delta H}$$

agrees well with the experimental data if we assume $H_2^* = 40$ Oe. An agreement between the calculated value of j_{ph} with the experimental data is obtained when the electron density in the 0^+ band is an order of magnitude less than the total density. This seems to be quite reasonable if we bear in mind the process of impact ionization with the ground level 000^+ by hot carriers.

SOME EXAMPLES OF OTHER PHYSICAL SYSTEMS IN WHICH AN INTERFERENCE RESONANT PHOTOCURRENT MAY APPEAR

1. Photocurrent in the case of resonant scattering by a quasistationary level

Some semiconductors may exhibit quasidecrete levels superposed on a continuous spectrum and these levels may be associated with excited states of deep structure defects,²² impurity complexes, or single impurity centers. Resonant scattering of photoelectrons by such levels also gives rise to the resonant photocurrents described above. We assume that an electron in the ground s state of an impurity is transferred under the influence of light to a band with an energy close to the quasistationary level energy ε_0 . The expression for the matrix element of such a transition considered to first order in the momentum is

$$M(\mathbf{k}, \omega) = \frac{e\mathbf{k}}{k^2} \left[M_1(\mathbf{k}, \omega) + \frac{\kappa\mathbf{k}}{k^2} M_2(\mathbf{k}, \omega) \right],$$

where \mathbf{e} is the polarization vector of light. The term $M_1(\mathbf{k}, \omega)$ corresponds to a dipole transition when the orbital momentum l of an electron in the band is 1, whereas the term $M_2(\mathbf{k}, \omega)$ corresponds to a quadrupole transition ($l = 2$). The absorption coefficient is proportional to $|M_1(\mathbf{k}, \omega)|^2$, while the photocurrent is proportional to the product $\text{Re}[M_1(\mathbf{k}, \omega)M_2^*(\mathbf{k}, \omega)]$. Resonant scattering gives rise to singularities in the matrix elements M_1 or M_2 . If the state of an electron at the level corresponds to the momentum $l = 1$ (p level), then a singularity appears in the

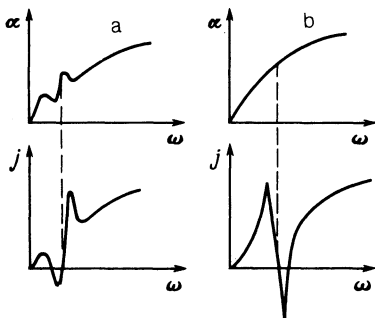


FIG. 12. Calculated spectral dependence of the absorption coefficient and of the photocurrent in the case of photoionization of an impurity level in a rectangular well, subject to resonant scattering by excited states of different symmetries.²² a) $l = 1, p$ level; b) $l = 2, d$ level.

spectral dependences of both the absorption coefficient and the photocurrent (Fig. 12). However, if the level corresponds to the orbital momentum $l = 2$ (d level), then the singularity arises in the matrix element M_2 so that a resonance appears only in the spectral dependence of the photocurrent. The profile of the resonant dependence $j_r(\omega)$ can be easily determined on the basis of the following considerations. If the frequency of light is close to a resonance in one of the channels (p or d), the matrix element corresponding to this channel is proportional to $1/(\Delta + i\Gamma)$, where Γ is the level half-width, while the scattering in the second channel is weak. Therefore, the spectral dependence $j_r(\omega)$ is the real part of $1/(\Delta + i\Gamma)$, i.e.,

$$j_r(\omega) \propto \Delta/(\Delta^2 + \Gamma^2).$$

2. Photocurrent due to a resonant interaction with an optical phonon

In all the preceding examples the resonant level appears superposed on the continuous spectrum of the semiconductor. An interference photocurrent may appear however even in such cases provided the levels are located within the band gap. Then, the resonant scattering of free electrons is due to the interaction with optical phonons. This situation has been investigated by Grimmeiss *et al.* in the specific case of the Fano resonances (see, for example, Ref. 23).

We shall assume that there are several energy levels in the band gap of a semiconductor and that they correspond to different impurities or to the ground and excited states of the same impurity (Fig. 13). Initially these electrons are at a level with the lowest energy ε_0 . Under the influence of a sufficiently high frequency, such that $\hbar\omega > |\varepsilon_0|$, they are transferred to the allowed band and a photocurrent proportional to κ is observed. The value of this current depends smoothly on ω everywhere with the exception of narrow intervals where the energy of the newly created electrons $\varepsilon_k = \varepsilon_0 + \hbar\omega$ is close to $\varepsilon_i + \hbar\omega_0$; here ε_i is the energy of one of the levels and $\hbar\omega_0$ is the energy of an optical phonon. In these intervals we can expect not only the direct $1 \rightarrow 3$ transitions to the band, but also transitions accompanied by the resonant scattering of electrons on the appropriate levels accompanied by the emission and subsequent absorption of an optical phonon ($1 \rightarrow 3 \rightarrow 2 \rightarrow 3$ transition in Fig. 13). Interference between the transitions gives rise to a Fano resonance and to a quantum-interference photocurrent. As already mentioned, the part of the interference term even in \mathbf{k} is

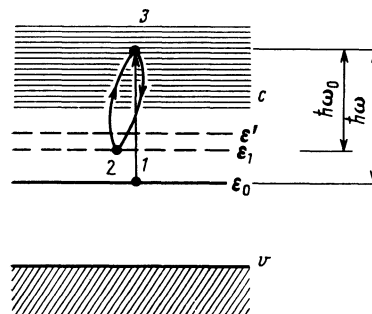


FIG. 13. Schematic representation of the formation of a resonant photocurrent due to photoionization of a deep center, allowing for the interaction with an optical phonon.

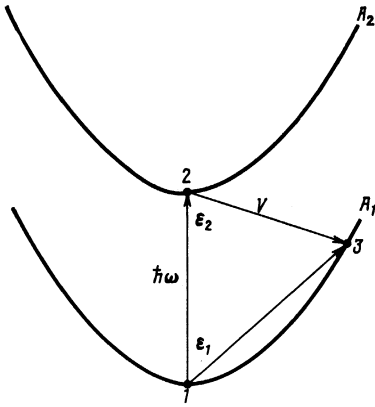


FIG. 14. Formation of a quantum-interference photodrift on absorption of light in a mixture of two gases. Here, A_1 and A_2 are the ground and excited states of the active gas; V is the interaction of the active and buffer gases.

responsible for an absorption resonance, whereas the odd part is responsible for a photocurrent resonance.

3. Quantum-interference photodrift in gases

So far we have considered the photocurrent in a semiconductor. However, a similar effect can occur also in other media, particularly in gases. Consider a mixture of two gases, one active A and the other buffer B . We assume that the frequency of light is close to a resonance for the transitions between the ground 1 and excited 2 states of molecules of the active gas (Fig. 14). The collisions of these molecules with those of the buffer gas may induce transitions as a result of which the molecules A still remain in the ground state, but acquire a kinetic energy

$$e_A = \frac{m_B}{m_A + m_B} \hbar\omega,$$

where m_A and m_B are the masses of molecules of the active and buffer gases, respectively. For $\hbar\omega \approx \epsilon_2 - \epsilon_1$, such transitions may occur in two ways: directly ($1 \rightarrow 3$) and via an intermediate excited state ($1 \rightarrow 2 \rightarrow 3$). Interference between the amplitudes of these transitions may give rise to a resonant drift of molecules of the active gas. It should be mentioned that in order to observe this effect experimentally, the $1 \rightarrow 2$ transition should be weakly allowed. Otherwise the effect may be masked by what is known as the light-induced drift.^{7,24,25}

We conclude by noting that quantum-interference photocurrents may be used as a new method for detection and determination of the parameters of energy levels in various physical systems. The advantage of such a method compared with the usual techniques (investigation of the optical absorption, photoconductivity, etc.) is that it can deal with a resonance signal whose amplitude is of the order of the background even if the relevant optical transition is almost forbidden. An analysis of the photocurrent curve can be used to determine practically all the main parameters of the investigated level.

APPENDIX 1

We first consider the drag photocurrent which is due to the ionization of an impurity level. It is clear that the expression for the probability of an electron transition to a state

with the momentum \mathbf{k} includes the photon momentum $\boldsymbol{\kappa}$ as a small correction to \mathbf{k} , i.e., $W = W_{\mathbf{k}+\boldsymbol{\kappa}}$. Therefore

$$\begin{aligned} \mathbf{j} | \propto \sum_{\mathbf{Q}_k} \mathbf{k} W_{\mathbf{k}+\boldsymbol{\kappa}} &= \sum_{\mathbf{Q}_k} \mathbf{k} (\nabla_{\mathbf{k}} W_{\mathbf{k}, \boldsymbol{\kappa}}) = \frac{\partial W}{\partial \epsilon_{\mathbf{k}}} \frac{d\epsilon_{\mathbf{k}}}{d\mathbf{k}} \sum_{\mathbf{Q}_k} \mathbf{k} \left(\frac{\mathbf{k}}{|\mathbf{k}|} \boldsymbol{\kappa} \right) \\ &= \frac{4\pi}{3} \boldsymbol{\kappa} \frac{\partial W}{\partial \epsilon_{\mathbf{k}}} \frac{d\epsilon_{\mathbf{k}}}{d\mathbf{k}} k. \end{aligned}$$

On the other hand, the absorption coefficient is described by

$$\alpha | \propto \sum_{\mathbf{Q}_k} W_{\mathbf{k}+\boldsymbol{\kappa}} = \sum_{\mathbf{Q}_k} W_{\mathbf{k}} = 4\pi W_{\mathbf{k}}.$$

A comparison of the expressions for j and α yields

$$j \propto d\alpha/d\epsilon_{\mathbf{k}} = d\alpha/\hbar d\omega.$$

This analysis can be applied, subject to small changes, also to the case when the photocurrent is due to transitions between two subbands, as reported for example in Refs. 7–9. The absorption of light then exhibits a resonance and we have

$$\alpha \propto \Gamma/(\Delta^2 + \Gamma^2).$$

Consequently,

$$j \propto d\alpha/\hbar d\omega = d\alpha/d\Delta \propto \frac{\Gamma\Delta}{(\Delta^2 + \Gamma^2)^2}$$

and if $\Delta \gg \Gamma$, we have $j \propto 1/\Delta^3$.

APPENDIX 2

A matrix element of the type

$$P_k = \frac{eA_1}{mc} \left\langle \varphi_k \left| \exp\left(\frac{i\boldsymbol{\kappa}z}{\hbar}\right) \hat{k}_- \right| \chi_0 \right\rangle$$

can be calculated directly if we use the equation

$$\hat{k}_- = -i \frac{m}{2^{1/2}\hbar} [\rho_-, \mathcal{H}],$$

where

$$\mathcal{H} = k^2/2m + V, \quad \rho_- = x - iy,$$

and V is the Coulomb potential of an impurity. Then, in the approximation linear in $\boldsymbol{\kappa}$, we obtain

$$\begin{aligned} \left\langle \varphi_k \left| \exp\left(\frac{i\boldsymbol{\kappa}z}{\hbar}\right) \hat{k}_- \right| \chi_0 \right\rangle &= \frac{i(\epsilon_k - \epsilon_+)m}{2^{1/2}\hbar} \langle \varphi_k | \rho_- | \chi_0 \rangle \\ &- \frac{\boldsymbol{\kappa}(\epsilon_k - \epsilon_+)m}{2^{1/2}\hbar^2} \langle \varphi_k | \rho_- z | \chi_0 \rangle - \frac{\boldsymbol{\kappa}}{2^{1/2}} \left\langle \varphi_k \left| \rho_- \frac{d}{dz} \right| \chi_0 \right\rangle, \end{aligned} \quad (2.1)$$

where ϵ_k and ϵ_+ are the energies of an electron in an allowed band and at an impurity.

The matrix elements on the right-hand side of Eq. (2.1) no longer vanish if we replace φ_k and χ_0 with the approximate functions of Eqs. (18) and (19). However, in calculating of the latter, namely $\langle \varphi_k | \rho_- d/dz | \chi_0 \rangle$, we are faced with the following difficulty. The momentum k corresponding to the final state is of the order of \hbar/a_H and, consequently, the main contribution to the integral comes from $z \sim a_H$. However, as pointed out in Ref. 20, the derivatives $d\varphi_k/dz$ and $d\chi_0/dz$ obtained in this region do not agree with the derivatives of the approximate functions (18) and (19). The use of more rigorous expressions for $d\chi_0/dz$ (or for $d\varphi_k/dz$) results in very involved calculations. Therefore, we proceed as follows.

We write down the Schrödinger equation for an electron in the band 0^+ and at the level 000^+ :

$$\frac{\hat{k}^2}{2m}|\chi_0\rangle + V|\chi_0\rangle = \varepsilon_+|\chi_0\rangle, \quad (2.2)$$

$$\langle\varphi_k|\frac{\hat{k}^2}{2m} + \langle\varphi_k|V = \varepsilon_k\langle\varphi_k|. \quad (2.3)$$

We now apply the operator $\exp(i\kappa z/\hbar)\hat{k}_-$ to Eq. (2.2) from the left and to Eq. (2.3) from the right, and take the difference of the resultant expressions. Then, applying the following commutation relationships

$$[\hat{k}_x, \hat{k}_-] = -\frac{i}{2^{1/2}}\left(\frac{\hbar}{a_H}\right)^2, \quad [\hat{k}_y, \hat{k}_-] = \frac{i}{2^{1/2}}\left(\frac{\hbar}{a_H}\right)^2,$$

we find that after simple transformations in the approximation linear in κ the result is

$$\begin{aligned} & \langle\varphi_k|\exp\left(\frac{i\kappa z}{\hbar}\right)\hat{k}_-|\chi_0\rangle \\ & = (\varepsilon_k - \varepsilon_+ + \hbar\omega_c)^{-1} \left(-\frac{i\hbar}{2^{1/2}} \langle\varphi_k|\frac{V}{r^2}\rho_-|\chi_0\rangle \right. \\ & \quad \left. + \kappa \frac{i}{2^{1/2}\hbar} (\varepsilon_k - \varepsilon_+) \langle\varphi_k|\rho_- \hat{k}_z|\chi_0\rangle \right). \end{aligned} \quad (2.4)$$

Equating now the terms proportional to κ on the right-hand sides of Eqs. (2.1) and (2.4), we can express $\langle\varphi_k|\rho_- d/dz|\chi_0\rangle$ in terms of $\langle\varphi_k|\rho_- z|\chi_0\rangle$. Consequently, we find that P_k is given by

$$P_k = i \frac{eA_T\omega}{2^{1/2}c} \left(1 - \kappa \frac{\omega}{2\omega + \omega_c} \frac{d}{dk} \right) \langle\varphi_k|\rho_-|\chi_0\rangle.$$

Here we use the law of conservation $\varepsilon_k - \varepsilon_0 = \hbar\omega$ and the fact that in the case of the function (19), we have

$$\langle\varphi_k|\rho_- z|\chi_0\rangle = i\hbar \frac{d}{dk} \langle\varphi_k|\rho_-|\chi_0\rangle.$$

The final expression for P_k was given earlier in the main text.

¹¹Strictly speaking, a change in the orientation of a sample and also reversal of the direction of κ results in some change in the profile of the resonances, which is particularly noticeable along the [111] direction. This is possibly due to the contribution of the photogalvanic current,¹⁶ which is even in δH and due to manifestation of a quantum-interference current in noncentrosymmetric crystals mentioned in the Introduction. However, reliable identification of the latter would require additional experiments.

²¹In fact, in our case both χ_0 and φ_k are spinors. We shall allow for this circumstance in specific calculations.

¹A. P. Dmitriev, S. A. Emel'yanov, Ya. V. Terent'ev, and I. D. Yaroshetskii, *Pis'ma Zh. Eksp. Teor. Fiz.* **49**, 506 (1989); **51**, 392 (1990) [*JETP Lett.* **49**, 584 (1989); **51**, 445 (1990)].

²A. P. Dmitriev, S. A. Emel'yanov, Ya. V. Terent'ev, and I. D. Yaroshetskii, *Solid State Commun.* **72**, 1149 (1989).

³U. Fano, *Phys. Rev.* **124**, 1866 (1961).

⁴A. M. Danishevskii, A. A. Kastal'skii, S. M. Ryvkin, and I. D. Yaroshetskii, *Zh. Eksp. Teor. Fiz.* **58**, 544 (1970) [*Sov. Phys. JETP* **31**, 292 (1970)].

⁵A. F. Gibson, M. F. Kimmitt, and A. C. Walker, *Appl. Phys. Lett.* **17**, 75 (1970).

⁶P. M. Valov, B. S. Ryvkin, S. M. Ryvkin *et al.*, *Fiz. Tekh. Poluprovodn.* **5**, 1772 (1971) [*Sov. Phys. Semicond.* **5**, 1545 (1971)].

⁷A. M. Dykhne, V. A. Roslyakov, and A. N. Starostin, *Dokl. Akad. Nauk SSSR* **254**, 599 (1980) [*Sov. Phys. Dokl.* **25**, 741 (1980)].

⁸E. M. Skok and A. M. Shalagin, *Pis'ma Zh. Eksp. Teor. Fiz.* **32**, 201 (1980) [*JETP Lett.* **32**, 184 (1980)].

⁹A. A. Grinberg and S. Luryi, *Phys. Rev. B* **38**, 87 (1988).

¹⁰E. L. Ivchenko and G. E. Pikus, *Problems in Modern Physics* [in Russian], Nauka, Leningrad (1980), p. 275.

¹¹B. D. McCombe and R. J. Wagner, *Proc. Eleventh Intern. Conf. on Physics of Semiconductors*, Warsaw, 1972, Vol. 1, publ. by PWN, Warsaw (1972), p. 321.

¹²F. Kuchar, R. Meisels, R. A. Stradling, and S. P. Najda, *Solid State Commun.* **52**, 487 (1984).

¹³Z. Barticevic, M. Dobrowolska, J. K. Furdyna, *et al.*, *Phys. Rev. B* **35**, 7464 (1987).

¹⁴S. D. Ganichev, S. A. Emel'yanov, and I. D. Yaroshetskii, *Pis'ma Zh. Eksp. Teor. Fiz.* **35**, 297 (1982) [*JETP Lett.* **35**, 368 (1982)].

¹⁵Yu. M. Burdukov and V. E. Sedov, *Kristallografiya* **13**, 556 (1968) [*Sov. Phys. Crystallogr.* **13**, 466 (1968)].

¹⁶L. I. Magarill, A. M. Palkin, V. N. Sozinov, and M. V. Éntin, *Zh. Eksp. Teor. Fiz.* **97**, 950 (1990) [*Sov. Phys. JETP* **70**, 533 (1990)].

¹⁷E. I. Rashba and V. I. Sheka, *Fiz. Tverd. Tela (Leningrad)* **3**, 1735 (1961) [*Sov. Phys. Solid State* **3**, 1257 (1961)].

¹⁸Y.-F. Chen, M. Dobrowolska, J. K. Furdyna, and S. Rodriguez, *Phys. Rev. B* **32**, 890 (1985).

¹⁹V. N. Abakumov and I. N. Yassievich, *Zh. Eksp. Teor. Fiz.* **61**, 2571 (1971) [*Sov. Phys. JETP* **34**, 1375 (1972)].

²⁰V. I. Perel' and D. G. Polyakov, *Zh. Eksp. Teor. Fiz.* **81**, 1232 (1981) [*Sov. Phys. JETP* **54**, 657 (1981)].

²¹V. F. Gantmakher and Y. B. Levinson, *Carrier Scattering in Metals and Semiconductors*, North-Holland, Amsterdam (1987) [*Modern Problems in Condensed Matter Sciences*, Vol. 19].

²²A. P. Dmitriev, É. Z. Imamov, and I. N. Yassievich, *Fiz. Tekh. Poluprovodn.* (in press) [*Sov. Phys. Semicond.* (in press)].

²³M. Kleverman, G. Grossmann, J. Olajos, and H. G. Grimmeiss, *Proc. Nineteenth Intern. Conf. on Physics of Semiconductors*, Warsaw, 1988, Vol. 2., Institute of Physics, Polish Academy of Sciences, Warsaw (1988) p. 979.

²⁴V. D. Antsygin, S. N. Atutov, F. Kh. Gel'mukhanov, *et al.*, *Pis'ma Zh. Eksp. Teor. Fiz.* **30**, 282 (1979) [*JETP Lett.* **30**, 261 (1979)].

²⁵H. G. C. Werij, J. E. M. Haverkort, and J. P. Woerdman, *Phys. Rev. A* **33**, 3270 (1986).

Translated by A. Tybulewicz